ORIGINAL ARTICLE

Application of silver nanoparticles toward Co(II) and Pb(II) ions contaminant removal in groundwater

Isaac Kwaku Attatsi[1,2,3] · Francis Nsiah[3]

Abstract

Applications of nanomaterials has recently been of keen interest to researchers. This fascinating drive ensued due to their unique properties such as optical, magnetic, ease of synthesis, large surface area, and tunable surface chemistry and functionalization that are remarkably different from that of the bulk material. In this work, silver nanoparticles were synthesized and characterized using UV–Vis spectroscopy and scanning electron microscopy. The UV–Vis spectra obtained showed absorption peak at 406 nm wavelength and scanning electron microscope reveals an image of size, 20 nm. The efficiency of our nanomaterial was first tested using standard solutions of cobalt and lead. A bathochromic shift in the absorption wavelength from 406 to 445 nm and from 406 to 458 nm for Cobalt(II) and Lead(II), respectively, indicates an adsorption has taken place. Adsorption characteristics of the nanoparticles evaluated at various incubation periods indicates a percent reduction in cobalt(II) from 33.13 to 53.34% and 79.9–92.92% for lead(II) from day 1–14. This indicates high removal efficiency for lead(II) than cobalt(II) in the proof of concept experiment. The results obtained further reveal that metal ion removal from complexes using silver nanoparticles is time-dependent. The effectiveness of our nanomaterial toward metal ion removal from groundwater was tested using inductively coupled plasma optical emission spectroscopy. The results obtained reveal removal efficiencies of 24% for cobalt and 77% for lead. It is important to note that metal ion concentrations reduced as the incubation periods increased. This is in line with the proof of concept experiment using complex solutions of cobalt and lead. Notably, the percent removal of cobalt was quite low compared to proof of concept experiment. These observations suggest a further research into understanding the adsorption characteristics of metal ions to the surface of nanomaterials in aqueous media.

Keywords AgNPs · Chemical reduction · UV–Vis absorption · Incubation · Groundwater

Introduction

Pollution of water bodies emanating from natural and anthropogenic sources has become a matter of concern to mankind (Giri and Qiu 2016; Li et al. 2012; Vodela et al. 1997). Among the wide diversity of pollutants affecting water resources, heavy metals have received considerable attention due to their high toxicity even at low concentrations (Gaur et al. 2014; Jameel et al. 2012; Marcovecchio

et al. 2007). Frontiers of research into the adverse effects of heavy metal pollution of water bodies has been enlarged in recent times due to the contaminant effects of these metals on plants and animal species. Clean water is essential to human health, but due to population growth and extended droughts; the world is facing formidable challenges in meeting rising demands for clean water (Fu and Wang 2011; Gaur et al. 2014; Larsen et al. 2016; Savage and Diallo 2005; Tiwari et al. 2008). Many technologies have been employed in water treatment, and these include ion exchange, reverse osmosis, reduction, precipitation and membrane filtrations. The major hitch and disadvantage to these technologies emanates from their operational and maintenance cost (Jadhav et al. 2015; Mutamim et al. 2013; Weng et al. 2008). Despite being costly, they are also related to generation of sludge. Monteagudo and co-workers in their work reported sludge disposal as another problem with most of these technologies (Monteagudo and Ortiz 2000; Suksabye et al. 2008).

✉ Isaac Kwaku Attatsi
5103171312@stmail.ujs.edu.cn

1 School of Chemistry and Chemical Engineering, Jiangsu University, Zhenjiang 212013, People's Republic of China

2 School of Environment and Safety Engineering, Jiangsu University, Zhenjiang 212013, People's Republic of China

3 Department of Chemistry, College of Agriculture and Natural Sciences, University of Cape Coast, Cape Coast, Ghana

This makes improving water quality a difficult task in areas where the risk of contamination is high (Pradeep and Anshup 2009). Recently, Chouler et al. (2018) reported on screen-printed paper microbial fuel cell biosensor for detection of toxic compounds in water. Though it has a very good detection capability, an important aspect to consider lies on removal efficiency. An alternative technique to microbial fuel cell biosensors which could both detect and remove with high efficiency is nanotechnology.

Nanotechnology is currently the solution to water and wastewater treatment (Dasgupta et al. 2017; Ghasemzadeh et al. 2014; Kunduru et al. 2017; Li et al. 2018; Madhura et al. 2018; Savage and Diallo 2005; Tiwari et al. 2008; Westerhoff et al. 2016; Zhang et al. 2016). Pradeep and co-workers in their work reported the significant progress that has been made to utilize the chemistry of nanomaterial in several ways to improve water quality (Pradeep and Anshup 2009). Qu and co-workers in their research confirmed Pradeep and Anshup's assertion that nanotechnology holds great potential in advancing water and wastewater treatment (Pradeep and Anshup 2009; Qu et al. 2013; Westerhoff et al. 2016). Tremendous attention has been focused on the application of nanostructured materials as adsorbents or catalyst in the removal of toxic and harmful substances from wastewater and air (Ding et al. 2005; Santhosh et al. 2016; Yang et al. 2006; Zhang et al. 2016). For example, Shankar and co-workers reported on using *chitosan* to remove pentachlorophenol pesticides from aqueous media (Shankar et al. 2020). Eltayeb and Khan (2019) designed a new and novel nanocomposite with CNTs and applied it as a sensor toward environmetal remediation of polutants especially lead(II) ions. Preparation of novel wave-like zirconium tungstate nanocomposite was used for ion-selective studies in aqueous media (Khan et al. 2019). This illustrates the potentials of nanoparticle in environmental remediation of pollutants. According to Elangovan et al. (2008), nanoparticle-based adsorption techniques have become versatile methods for removal of metallic pollutants from aqueous solutions. The very small particle size nature (1–100 nm) of nanoparticles makes them extremely versatile remediation tools (Awual 2016). Apart from their size, they can also be magnetized and also attached onto solid matrix such as activated carbon which allows them to be attached to heavy metals (Agarwal and Joshi 2010). The technique has been so effective that even at very low concentrations, metallic ions could be removed (Azimi et al. 2017; Kogan et al. 2006; Shim and Gupta 2007). Agarwal and Joshi (2010) in their work reported reactive nanoparticles appear to be useful in remediating groundwater and thus may prove useful in removing pesticides, herbicides and heavy metals in the environment (Agarwal and Joshi 2010). Baldovi et al. used nanomaterials to understand the origin of the photocatalytic CO_2 reduction which was earlier reported in aqueous media (Baldoví

et al. 2015). The applications and removal efficiencies of nanoparticles make it a versatile technology for the present environmental remediations.

This work herein investigates and scout the practicability of the use of silver nanoparticles (AgNPs) in the removal of metal ion contaminants in groundwater samples in the Cape Coast Metropolis, Ghana. The sequence adopted in this work involves the synthesis and characterization of silver nanoparticles which was followed by a proof-of-concept experiment where we tested the efficacy of our nanoparticles using standard solutions of cobalt and lead at varied periods of incubation. Finally, we applied our nanomaterial to groundwater where we confirmed their effective capabilities toward metal ion contaminate removal.

Materials and methods

Study areas

Cape Coast Metropolis, a coastal town, with its scarcity of running tap water during the dry seasons was chosen for this research. Assin Fosu (in-land town) was chosen as a control to compare if there could be wide difference in metal ion concentrations between coastal and in-land town. From the map, longitude 1° 11′ 41″ W and latitude 5° 07′ 20″ N defines the location of Cape Coast metropolis as shown in Fig. 1a. Assin Fosu in the Assin North district of the Central Region lies within longitude 1° 25′ 41″ W and latitude 6° 05′ 20″ N of the Central Region of Ghana (Fig. 1b). All samples were taken from the main source of water (groundwater) supply which are suspected to have elevated amount of heavy metals due to the environment these wells are found.

Materials and reagents

UV–Vis spectra were measured using a T70 UV–Vis spectrophotometer (PG Instrument Ltd). Varian 715-ES inductively coupled plasma–optical emission spectroscopy was used for the quantitative analysis of cobalt(II) and lead(II) ions. Field emission scanning electron microscope with model number S4800 FE-SEM system (Hitachi Scientific Equipment, Japan) equipped with an ultrahigh resolution and low voltage 10 kV SEM inspection with advanced sample navigation package was used to characterize the morphology. Centrifuge (model 0257-210) from Wagtech International Limited, UK, was used to separate the adsorbent and treated water. All chemicals such as $AgNO_3$, $NaBH_4$, HNO_3, and cobalt and lead standards for ICP-OES were purchased from Merck (Darmstadt, Germany) and were of analytical grade and used without any further treatment unless otherwise stated. Standard solutions of lead and cobalt were
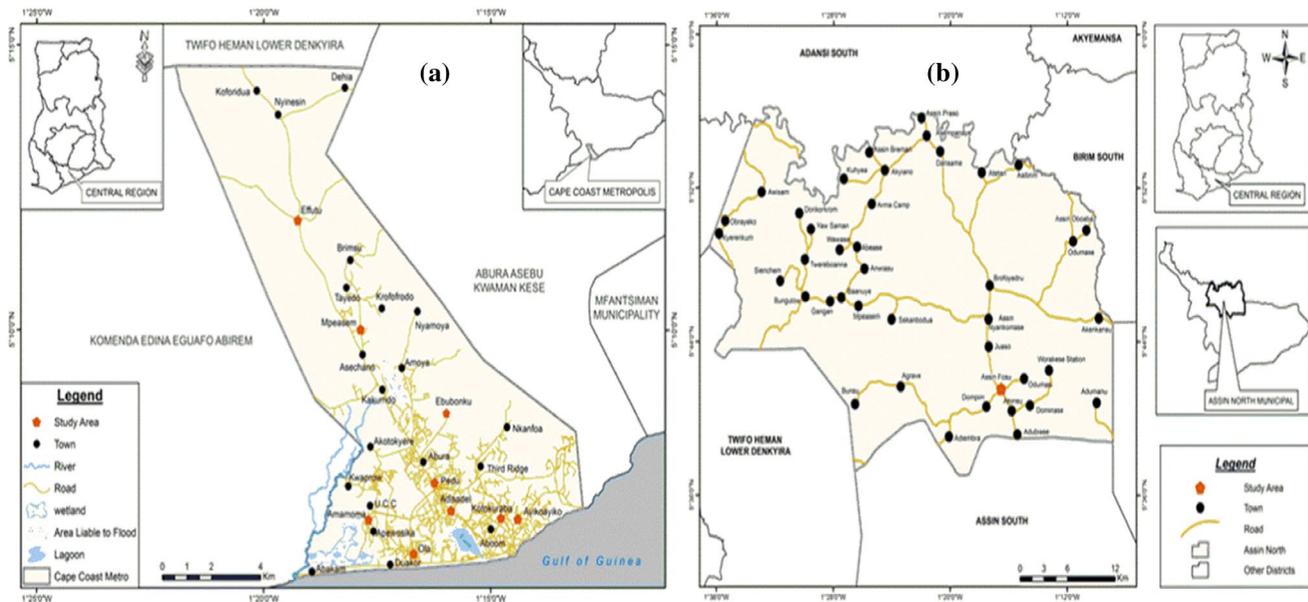
Fig. 1 Map showing the areas of study in **a** Cape Coast Metropolis and **b** Assin Fosu in the Central Region of Ghana. The study areas are indicated in red color

prepared using modified procedures as stated. All solutions were prepared using doubly distilled deionized water.

Sample collection, treatment and storage

Groundwater samples were taken from 10 sampling sites. Selected sampling sites from Cape Coast Metropolis were Kotokuraba, Mpeasem, Amamoma, Effutu, Adisadel, OLA, Ebubonku, Ayikoayiko and Pedu; a control sample from Assin Fosu in the Assin North district of the Central Region of Ghana. Nitric acid-treated 1 L polyethylene bottles were used for sampling to prevent traces of metals leaching into the water samples. In addition, nitric acid treatment procedure was intended to preserve trace metals from microbial activity and adsorption losses to the walls of the sample container (Biziuk et al. 2009; Federation and Association 2005; Shugar et al. 2001; Sundaram et al. 2009). The temperature and pH values for the samples recorded were 29 °C and pH units 2.0. Samples were transported and stored in the refrigerator at 4 °C. This is to minimize sample losses through evaporation and any possibility of chemical conversion (Federation and Association 2005).

Synthesis of silver nanoparticles (AgNPs)

AgNPs utilized in this study were synthesized using the method proposed by Mulfinger and co-workers (Mulfinger et al. 2007). The method involved the reduction of Ag^+ to Ag^0. In this synthetic process, 1.0 mM $AgNO_3$ was continually added to 2.0 mM $NaBH_4$ with continuous stirring for about 20 min on an ice bath. Formation of AgNPs was observed by a change in the color of the mixture from colorless to yellow. The UV–Vis characterization showed the absorption peak of our nanomaterial at 406 nm. Morphological characterization revealed a nanomaterial of size 20 nm which is in line with literature (Mulfinger et al. 2007). To determine the concentration of the synthesized AgNPs, Eqs. (1) and (2) were used which indicated the concentration of our nanomaterial is 4.06×10^{-7} mol/L. Equation (1) gives the number of atoms per nanoparticle which is substituted into Eq. (2) to obtain the concentration of the prepared AgNPs.

$$N = \frac{\pi \rho D^3 N_A}{6M} \tag{1}$$

N = number of atoms per nanoparticle, ρ = density of face centered cubic (fcc) silver = 10.5 g/cm^3 (1.05×10^{-20} g/nm^3), D = average diameter of nanoparticles = 20 nm, M = atomic mass of silver = 108 g/mol, N_A = number of atoms per mole = 6.02×10^{23} atoms/mol

$$C = \frac{N_T}{N V N_A} \tag{2}$$

C = molar concentration of nanoparticle solution, N_T = Total number of silver atoms added in $AgNO_3$ = 1.20×10^{20} atoms, N = number of atoms per nanoparticle (determined in Eq. 2), V = volume of the reaction solution = 2×10^{-3} L, N_A = number of nanoparticles per mole.
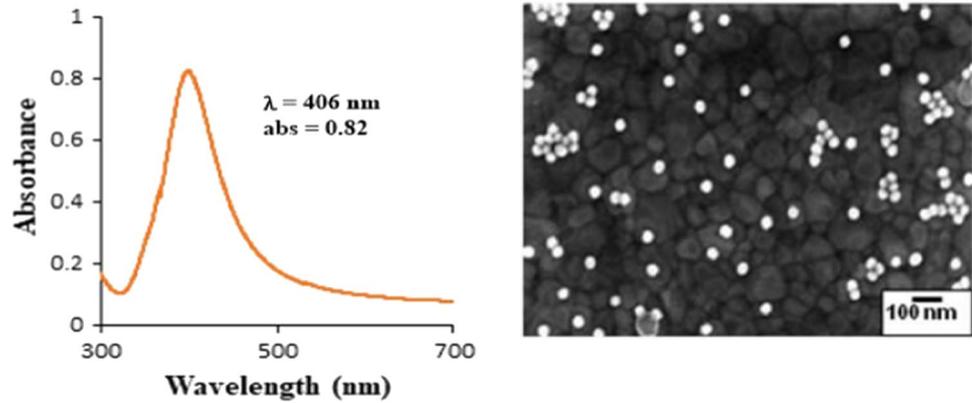
Treatment of standard solutions (cobalt and lead) and groundwater samples using AgNPs

Prior to the treatment of standards with AgNPs, standard solutions of cobalt and lead were prepared according to APHA (American Public Health Association) method (Federation and Association 2005). Dilute concentrations of 5, 10, 15, 20 and 25 µg/mL were prepared from the standard stock solutions. To 10 mL portions of these dilute solutions, 0.5 mL portions of AgNPs were added. The incubation period used in this work were 1 day, 3 days, 5 days, 7 days and 14 days. All solutions were centrifuged at 3000 rpm for 10–20 min, and the supernatant portions taken for UV–Vis analysis. Absorbance measurements for both solutions were taken at 510 nm wavelength. Digested groundwater samples were treated with 0.5 mL portions of AgNPs and incubated using the same process as described for the metal standard solutions. Quantitative determinations of metal ion concentrations were carried out using inductively coupled plasma-optical emission spectrophotometer (ICP-OES). This is to
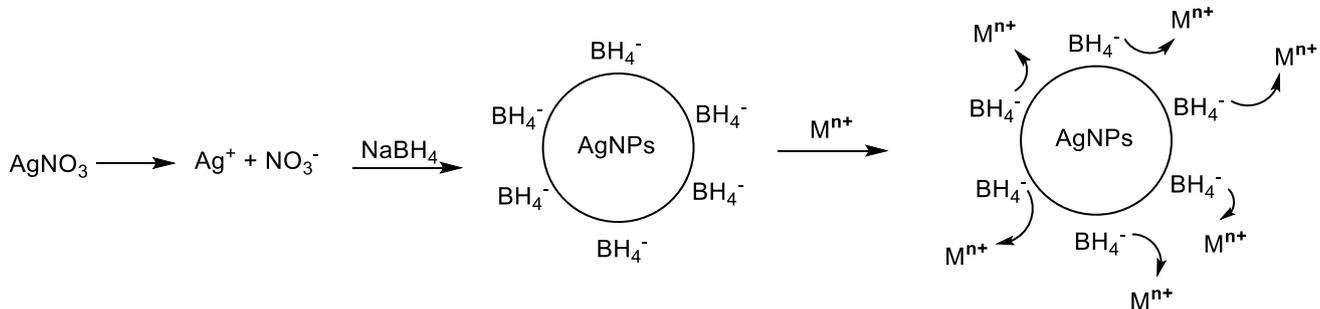
Scheme 1 Proposed mechanism showing how the metal-ions were adsorbed to the surface of AgNPs
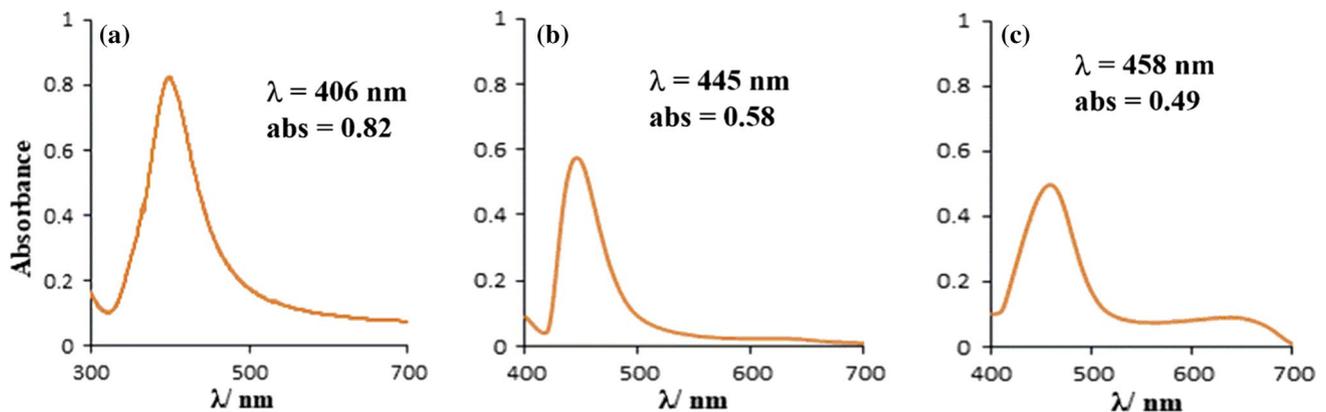

Fig. 3 UV–Vis absorption spectra for 20 nm AgNPs (**a**) bathochromic and hypochromic shift upon adsorption of cobalt (**b**) and lead solution (**c**) to AgNPs

determine the amounts of cobalt (Co^{2+}) and lead (Pb^{2+}) ions removed by the nanomaterial through adsorption. The selected ICP-OES emission wavelengths for cobalt and lead were 238.892 and 220.353 nm, respectively.

Results and discussion

UV–Vis spectroscopy and SEM characterization of AgNPs

Noble metal nanoparticles exhibit strong UV–Vis absorption band which is absent in the bulk metal. The major drive behind application of UV–Vis in this work is to identify wavelength changes upon surface modification of the nanoparticles. The measured UV–Vis absorption spectra of our nanoparticle fell in the range of 300–700 nm as shown in Fig. 2, (left). The material showed distinctive surface plasmon absorption peak at 406 nm, which is a characteristic of AgNPs. Morphological characterization of AgNPs (Fig. 2, right) showed particles of small sizes (20.3 ± 0.8 nm) with spherical shapes.

Metal–ions adsorption effects on surface plasmon band of AgNPs

After a successful synthesis and characterization of AgNPs, a proof of concept experiment was carried out to ascertain shift in the plasmon band upon surface modification. In this experiment, 0.5 mL of AgNPs was added to about 10 mL cobalt and lead standard solutions. The shift patterns observed upon interaction between silver nanoparticles and metal ions from cobalt and lead solutions are shown in Fig. 3. A remarkable redshift from 406 to 445 nm upon adsorption of cobalt(II) ions onto the surface of AgNPs was observed (Fig. 3b). Adsorption of lead(II) ions, on the other hand, showed an outstanding higher bathochromic shift from 406 to 458 nm as indicated in Fig. 3c. These redshifts as shown in Fig. 3b, c demonstrate changes in the optical properties of the nanoparticles following the adsorption of Co^{2+} and Pb^{2+} ions. Hypochromic shifts which were also observed further stipulates the surface modifications of the silver nanoparticles. A proposed mechanism was developed showing the adsorption of metal ions to the surface of the
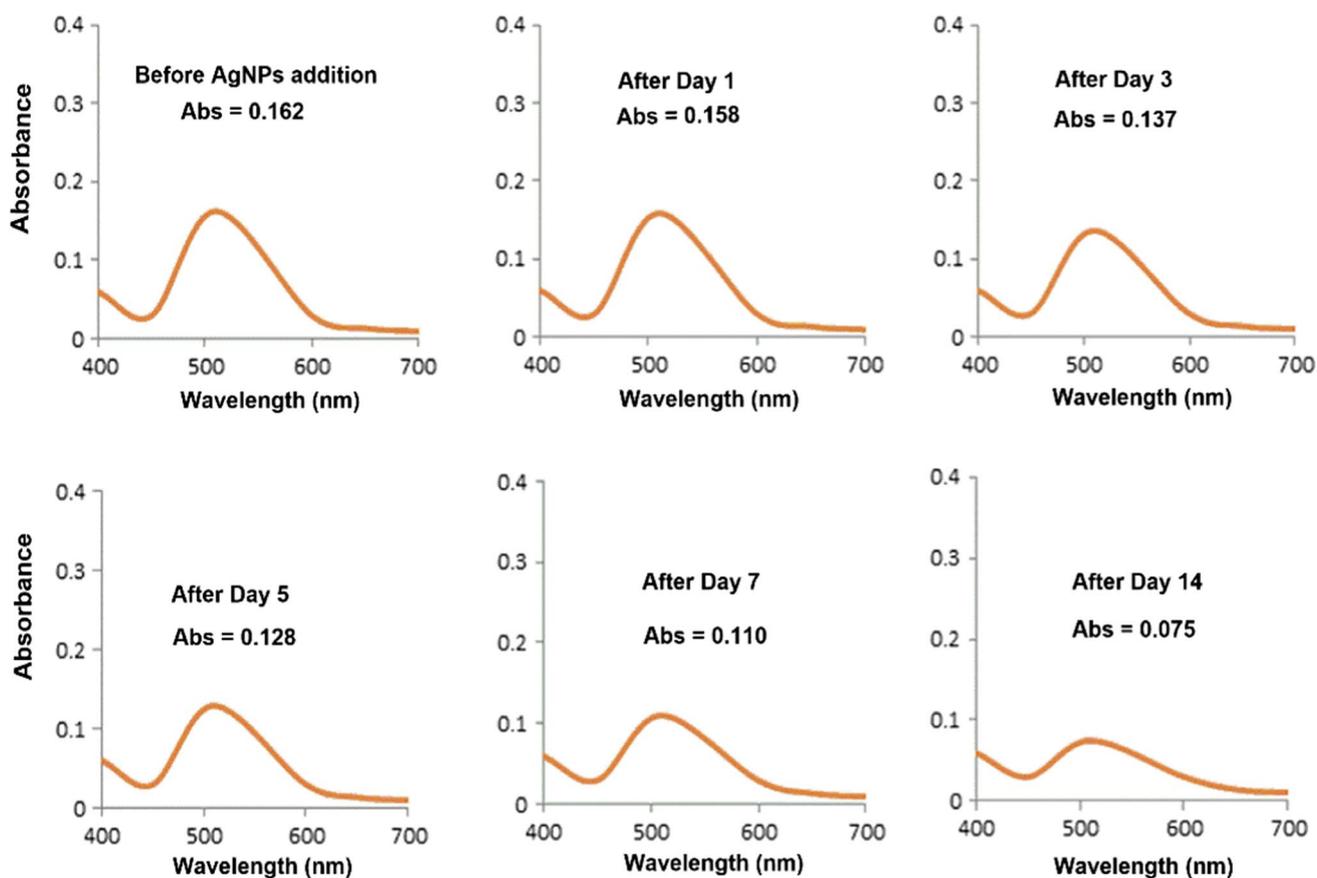

Fig. 4 UV–Vis spectrophotometric analysis showing AgNPs adsorption of 5 μg/mL cobalt(II) ions at 510 nm before and after addition of silver nanoparticles. The incubation period is 1–14 days

silver nanoparticles which change the surface morphology of the silver nanoparticle (Scheme 1).

Our results presented herein suggest the importance of UV–Vis spectrophotometry in tracking optical properties of nanoparticles upon surface modification. Based on these experimental facts, UV–Vis spectrometry was used to identifiably determine the level of reduction of metal ions from various concentrations of metal standards. In other to achieve this, silver nanoparticles effects before and after days of incubation were studied using 5–25 µg/mL cobalt(II) and lead(II) ion solutions recorded at 510 nm wavelength using UV–Vis spectroscopy technique. Figures 4 and 5 show the UV–Vis spectra of 5 and 25 µg/mL cobalt(II) ion solutions, while Figs. 6 and 7 show that of 5 and 25 µg/mL lead(II) ion solutions before and after days of incubation. The spectra obtained for all the metal ions concentrations (5–25 µg/mL) used for this experiment before and after nanoparticle incubation are summarized in Tables 1 and 2. As stated earlier in this manuscript, the adsorption of cobalt and lead ions to the surface of AgNPs could result in the decrease in the absorbance intensities an indicative of cobalt and lead ion removal (Sumesh et al. 2011; Yantasee et al. 2007). According to Ball, the decrease in absorbance intensities

depicts a decrease in concentration which is consistent with Beer–Lambert's law indicating the removal of metal ion in solution (Ball 2006).

It is important to reiterate that decrease in absorbance correlates with increase in the incubation period suggesting longer incubation period enhances removal efficiencies as shown in Fig. 8. The absorbance values measured at 510 nm for cobalt and lead were converted to percentages using Eq. (3) and the values shown in Tables 3 and 4 respectively.

$$\% M^{n+} \text{ removed} = \frac{(A_o - A_1)}{A_o} \times 100\% \tag{3}$$

where $\% M^{n+}$ = percent of metal ion, A_o = absorbance before nanoparticle addition, A_1 = absorbance after nanoparticle addition.

UV–Vis measurements from Tables 1 and 2 indicated a decrease in absorbance measurements for Co^{2+} and Pb^{2+} solutions as the incubation periods increase an indicative of greater adsorption of metal ion to the surface of the nanoparticles. This observation gave indication that our AgNPs could possibly remove Co^{2+} and Pb^{2+} in an aqueous environment. The data obtained from the spectra were converted to
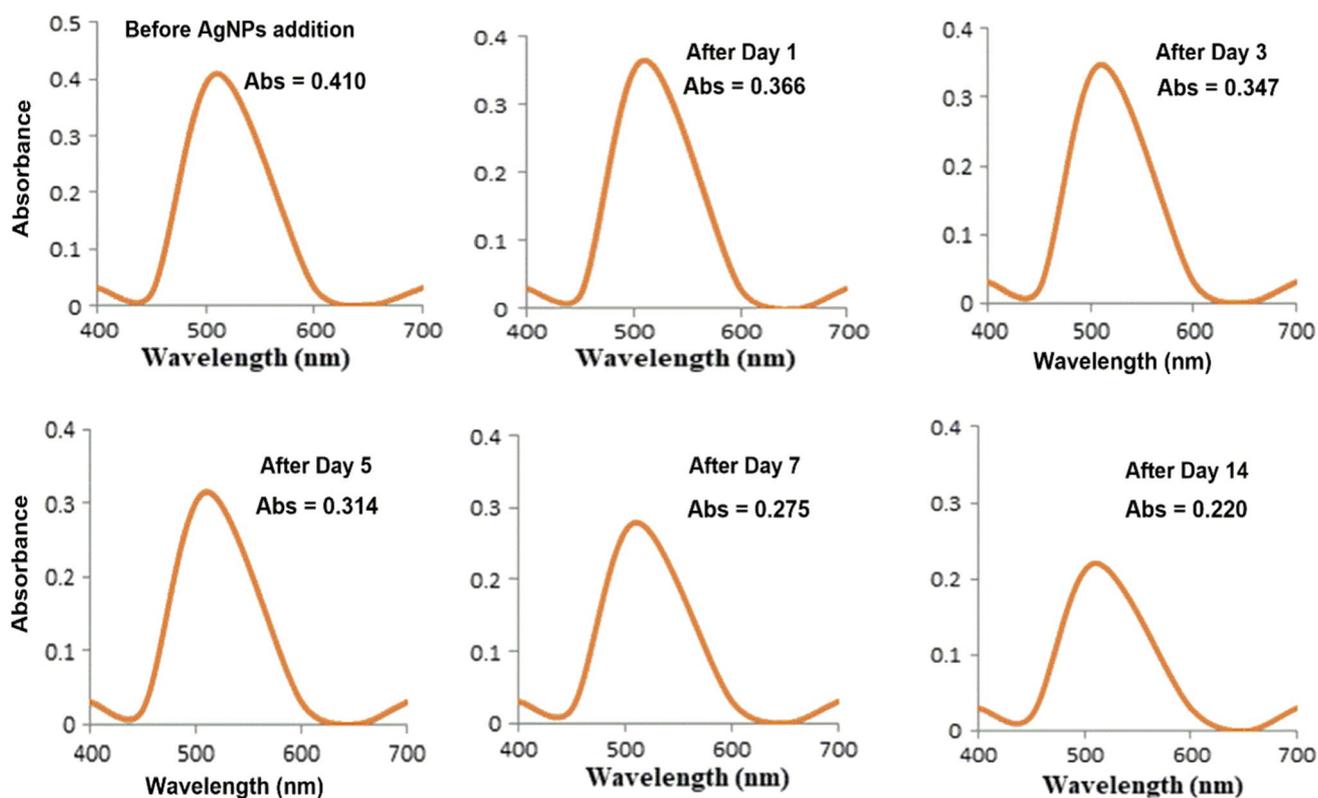

Fig. 5 UV–Vis spectrophotometric analysis showing AgNPs adsorption of 25 µg/mL cobalt(II) ions at 510 nm before and after addition of silver nanoparticles. The incubation period is 1–14 days

percentage, and this is shown in Table 3. At concentrations of 5, 10, 15, 20 and 25 µg/mL, the percent reductions on day 1 were 2.41, 7.16, 1.62, 13.23 and 10.53, respectively. Days 3, 5 and 7 also showed some percent reduction, but the highest percent reductions were observed on day 14. Co^{2+} solution treatment on day 14 showed 53.34% for the 5 µg/mL, 40.29% for 10 µg/mL, 33.13% for 15 µg/mL, 36.72% for 20 µg/mL and 46.18% for 25 µg/mL. This observation is consistent with the studies conducted by Alqudami et al. and Alissawi et al. which confirmed that metal ion adsorption to nanoparticles is time-dependent (Alissawi et al. 2013; Alqudami et al. 2013). Critical observation of results in Table 3 showed apart from 5 µg/mL, the removal efficiencies for 10, 15, 20 and 25 µg/mL were below 50%. This could mean a higher molar concentration for the AgNPs will be the most preferred for concentrations higher than 5 µg/mL than the one used whose concentration is 0.0438 ppm (4.06×10^{-7} mol/L) as determined from Eq. 2. Pb^{2+} complex solutions of 5, 10, 15, 20 and 25 µg/mL when incubated with 0.5 mL of AgNPs from days 1, 3, 5, 7 and 14 showed a trend indicating that the absorbances reduced as the

number of days increased (Alissawi et al. 2013; Alqudami et al. 2013). These observations as shown in Table 2 also confirm the ability of AgNPs to remove lead. As presented in Table 4, the maximum percent reduction was recorded for all the concentrations on day 14. Thus 5, 10, 15, 20 and 25 µg/mL had the concentrations of Pb^{2+} in the complex reduced by as low as 88.56, 92.92, 84.10, 80.11 and 79.92%, respectively, which are much higher than the percentages of Co^{2+} removed on the same day with the same amount of AgNPs applied. This high level of adsorption illustrates our nanomaterial is highly efficient and best choice for Pb^{2+} removal (Shiri-Yekta et al. 2013). The time dependency of nanoparticles as indicated by Alqudami et al. (2013) and Alissawi et al. (2013) was once again proven by our system. The time dependence of nanoparticle adsorption effects in Pb^{2+} solution is illustrated in Fig. 8 which illustrates AgNPs is a potential candidate for metal ion contaminants removal in groundwater samples.
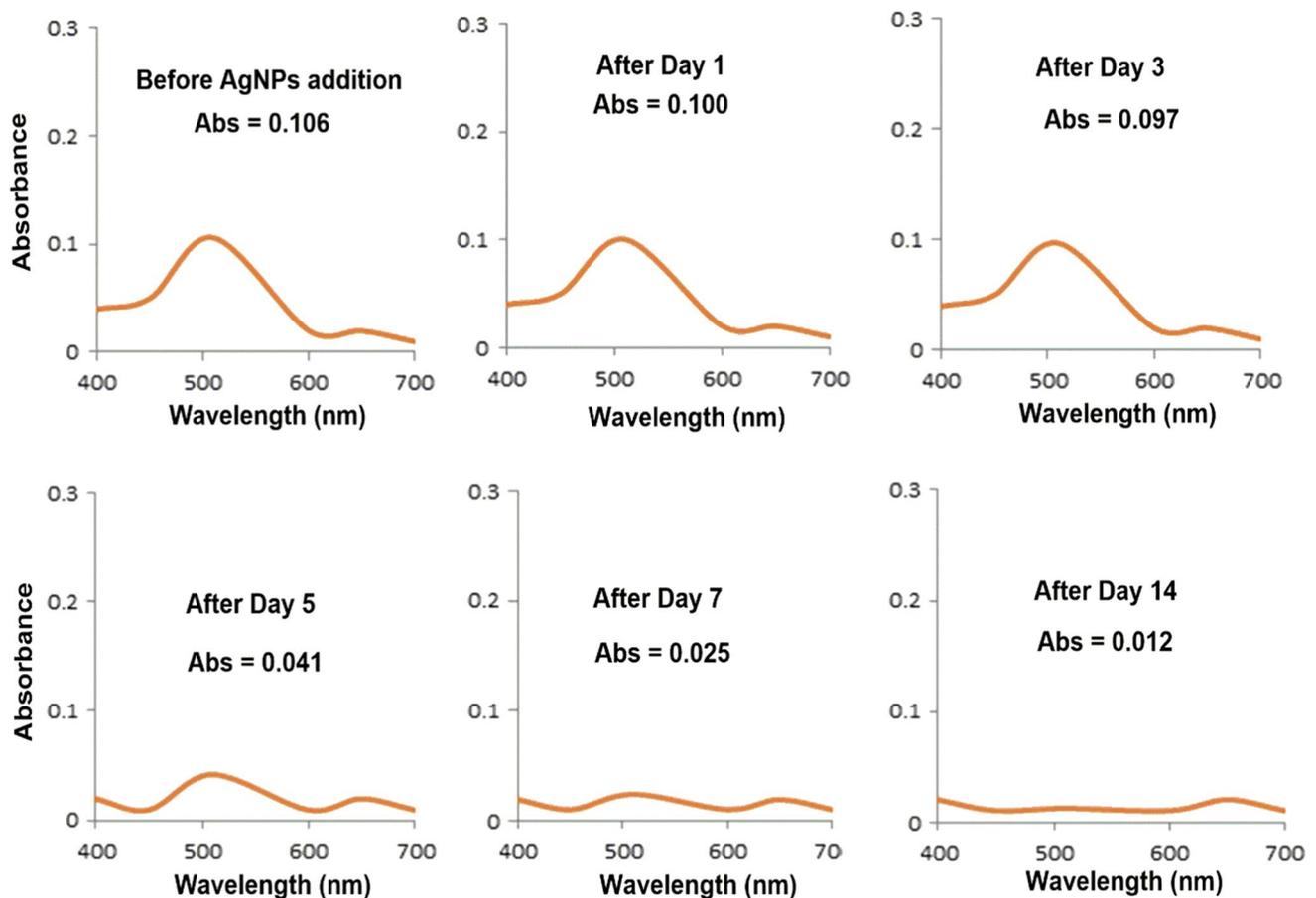

Fig. 6 UV–Vis spectrophotometric analysis showing AgNPs adsorption of 5 µg/mL lead(II) ions at 510 nm before and after addition of silver nanoparticles. The incubation period is 1–14 days
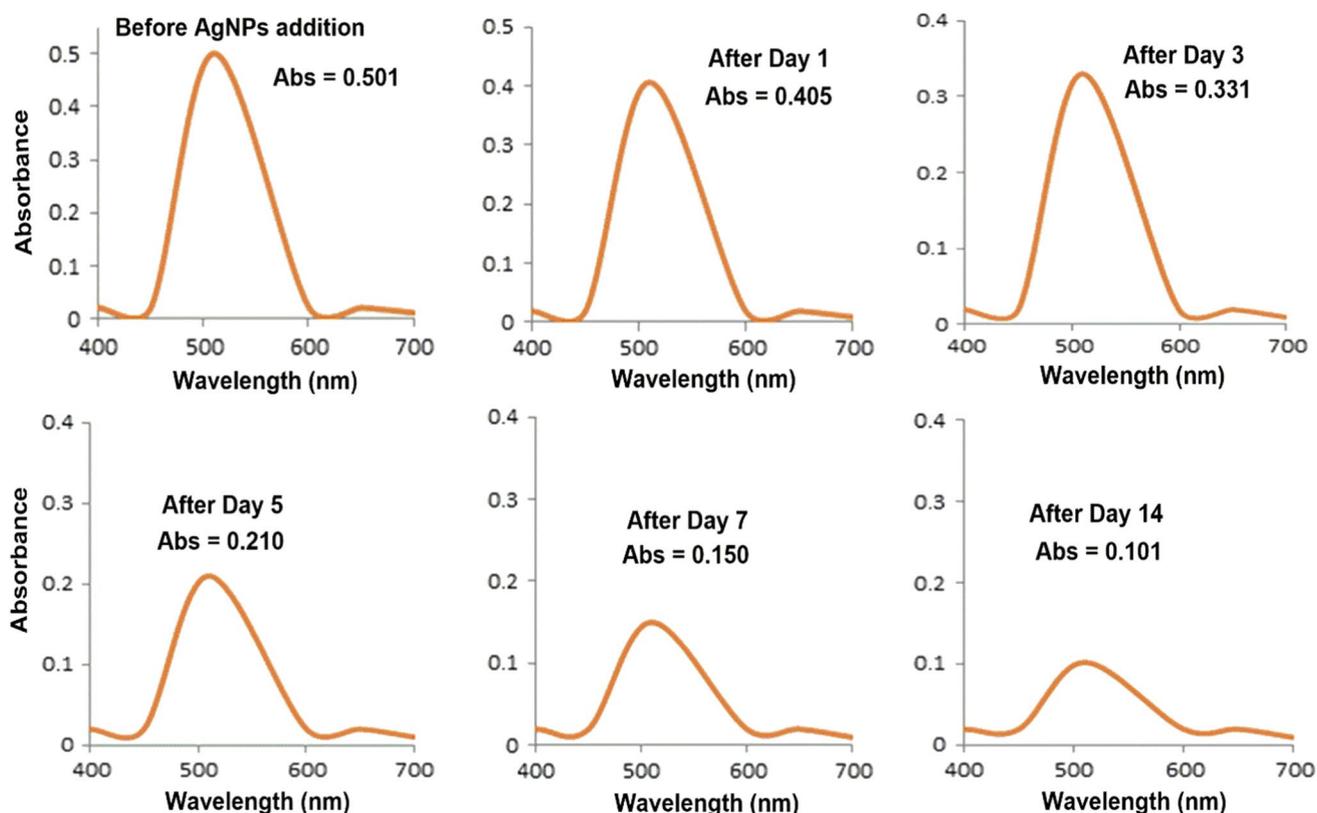
Fig. 7 UV–Vis spectrophotometric analysis showing AgNPs adsorption of 25 μg/mL lead(II) ions at 510 nm before and after addition of silver nanoparticles. The incubation period is 1–14 days

Quantitative determination of Co^{2+} and Pb^{2+} ions in groundwater samples

Since the key objective of this study was to remove Co^{2+} and Pb^{2+} ions from selected groundwater/wells, there was the need to apply a quantitative methodology to help determine amounts of metal ions removed within the samples. ICP–OES technique was used to determine the amounts of metal ions removed. Firstly, ten (10) samples from our 10 sampling sites were analyzed using ICP–OES to provide a baseline for comparison as shown in Table 5. It is observed that Co^{2+} ion levels in

all samples ranged between 0.133 and 0.146 ppm which are higher than the WHO allowable value of 0.01 ppm (Federation and Association 2005). Lead(II) ion concentrations obtained from the same 10 samples (Table 5) fell within 0.012 (Ebubonku)–0.185 (Amamoma) ppm range. Pb^{2+} concentrations in exception of Ebubonku samples exceeded the WHO permissible level of 0.015 ppm for potable water (Federation and Association 2005). Logical reasons attributed to these high Co^{2+} and Pb^{2+} ion concentrations from the results obtained may be due to pollution from vehicular movement within its vicinity and leachates from nearby automobile repair shops (Ajah et al.

Table 1 Absorbance of Co(II) solutions at 510 nm using AgNPs

Co(II) conc. (μg/mL)	Absorbance before AgNPs addition	Day 1	Day 3	Day 5	Day 7	Day 14
5	0.1617	0.1578	0.1371	0.1281	0.1100	0.0754
10	0.2318	0.2152	0.1948	0.1812	0.1556	0.1384
15	0.2768	0.2723	0.2495	0.2327	0.2152	0.1851
20	0.3230	0.2803	0.2721	0.2678	0.2590	0.2044
25	0.4095	0.3664	0.3471	0.3135	0.2754	0.2204

Absorbance measurements reported are the average values for 3 measurements and the standard deviations of all the spectral measurements were lower than 0.003 a.u.

Table 2 Absorbance of lead(II) solutions at 510 nm using AgNPs

Pb(II) conc. (µg/mL)	Absorbance before AgNPs addition	Day 1	Day 3	Day 5	Day 7	Day 14
5	0.1058	0.1003	0.0973	0.0413	0.0252	0.0121
10	0.1937	0.1462	0.1212	0.0643	0.0385	0.0137
15	0.3004	0.2112	0.2021	0.1070	0.0642	0.0477
20	0.3957	0.3045	0.2353	0.1537	0.1009	0.0787
25	0.5005	0.4047	0.3304	0.2101	0.1500	0.1005

Absorbance measurements reported are the average values for 3 measurements and the standard deviations of all the spectral measurements were lower than 0.003 a.u

2015; Odoh et al. 2011). It is important to note that Assin Fosu recording the highest Co^{2+} concentration debunk the notion that sample sites closer to the sea might have higher concentrations. Another confirmation of the above statement is shown in Pb^{2+} concentrations where apart from Amamoma, (coastal zone) the areas away from the sea (Effutu, Mpeasem, and Assin Fosu) still exhibited higher levels of lead meaning sea water intrusion may have very little or no effect on detectable metal ions from groundwater. Table 6 shows the mean values of three different ICP-OES analysis results of groundwater samples after AgNPs incubation from 24 h to 14 days. The choice of these incubation periods is to mimic the procedure employed in the analysis of standard solutions of Co^{2+} and Pb^{2+} ions presented earlier in this paper. Comparing the results in Tables 5 and 6, it can be concluded that the addition of AgNPs to the samples reduced the metal ion concentrations from the samples as indicated by a decrease in metal ion concentrations. The percent reductions of the various metals in each respective sample were computed relative to Tables 5 and 6 using Eq. (3) and shown in Table 7. The computation from kotokuraba samples shows a reduction percent of cobalt from 1.20, 4.16,

Table 3 Percent of Co(II) ions removed by AgNPs in different concentrations of Co(II) solutions

Co(II) conc. (µg/mL)	Day 1	Day 3	Day 5	Day 7	Day 14
5	2.41	15.21	20.78	31.97	53.34
10	7.16	15.96	21.82	32.87	40.29
15	1.62	9.89	15.93	22.25	33.13
20	13.23	15.76	17.09	19.81	36.72
25	10.53	15.24	23.44	32.75	46.18

All values reported here on the average have standard deviations below $\pm 0.05\%$

6.02, 19.16 and 20.58% on days 1, 3, 5, 7 and 14, respectively. Pb^{2+} ion percent reduction from same Kotokuraba samples were 8.83, 24.70, 32.30, 47.66 and 48.32% on days 1, 3, 5, 7 and 14, respectively. These results show a pattern indicative of reduced concentrations from day 1 to day 14. Although the percent reductions were minimal, we can say that the AgNPs were able to reduce metal ions that were initially contained in the samples. Further observation of Table 7 reveals that Mpeasem samples showed maximum removal efficiencies at 15.45% and 72.55% for Co^{2+} and Pb^{2+} ions, respectively. Assin Fosu, the controlled sample site also showed Co^{2+} ion concentrations reduced from 8.14% in day 1 to 24.02% on
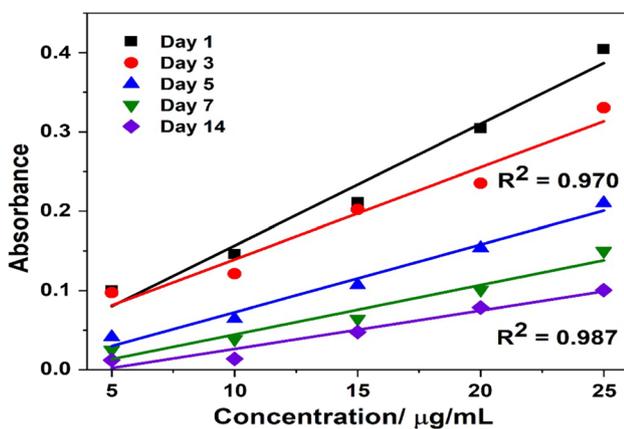
Table 4 Percent of Pb(II) ions removed by AgNPs in different concentrations of Pb(II) solutions

Pb(II) conc. (µg/mL)	Day 1	Day 3	Day 5	Day 7	Day 14
5	5.20	8.03	60.96	76.18	88.56
10	24.45	37.43	66.80	80.12	92.92
15	29.60	32.63	64.33	78.60	84.10
20	23.05	40.54	61.16	74.50	80.11
25	19.14	33.99	58.02	70.03	79.92

All values reported here on the average have standard deviations below $\pm 0.05\%$

Fig. 8 A plot showing nanoparticle effect on Pb^{2+} after 1–14 days of incubation. Maximum reductions were achieved in the 14th day

Table 5 Determination of the amounts of Co^{2+} and Pb^{2+} ions in groundwater samples before treatment with AgNPs

Sample sites	Co (ppm)	Pb (ppm)
Kotokuraba	0.133	0.146
Mpeasem	0.137	0.168
Amamoma	0.137	0.185
Effutu	0.139	0.170
Adisadel	0.142	0.138
Ebubonku	0.138	0.012
Ayikoayiko	0.132	0.096
Pedu	0.131	0.107
OLA	0.130	0.103
Assin Fosu	0.146	0.156

Concentrations shown are the mean of 3 replicates with standard deviations within ± 0.005 ppm

day 14. Pb^{2+} ion concentration also reduced from 1.38% on day 1 to 50.63% on day 14. Detailed observation of Table 7 further showed the highest Co^{2+} and Pb^{2+} ions

percent concentration removed were 24.02% (Assin Fosu) and 77.19% (Amamoma), respectively, on the 14th day of incubation. It can be generally stated that AgNPs were effective toward removal of Pb^{2+} than Co^{2+} ions. This observation was same in the proof of concept experiment where the percent Pb^{2+} (Table 4) removed were higher than Co^{2+} (Table 3) on day 14, respectively. This could mean there are other substances in the Co^{2+} solution that the nanoparticle has more affinity for and hence adsorbed them leaving a less surface area for the target ions adsorption implying that AgNPs may work effectively as Pb^{2+} ion removal in aqueous media than Co^{2+}. It could also suggest that a higher AgNPs concentration than the one prepared might be more effective toward the removal of the Co^{2+} ions in solution. It is important to note that AgNPs removal efficiencies as observed in the proof of concept experiment were higher than those recorded for groundwater samples. The result though not as expected is still considerable owing to the complex nature of groundwater analysis. We also want to reiterate that metal ion adsorption begins immediately after AgNPs were added

Table 6 Determination of the amounts of Co^{2+} and Pb^{2+} ions in groundwater samples after treatment with AgNPs

Sample sites	Days	Co/ppm	Pb/ppm	Sample sites	Days	Co/ppm	Pb/ppm
Kotokuraba	1	0.132	0.133	Ebubonku	1	0.134	0.105
	3	0.128	0.110		3	0.130	0.103
	5	0.125	0.099		5	0.116	0.102
	7	0.108	0.076		7	0.110	0.063
	14	0.106	0.075		14	0.109	0.059
Mpeasem	1	0.136	0.113	Ayikoayiko	1	0.128	0.094
	3	0.126	0.097		3	0.125	0.087
	5	0.121	0.063		5	0.122	0.086
	7	0.118	0.058		7	0.121	0.078
	14	0.116	0.046		14	0.120	0.072
Amamoma	1	0.132	0.168	Pedu	1	0.124	0.106
	3	0.123	0.143		3	0.121	0.088
	5	0.119	0.128		5	0.120	0.085
	7	0.115	0.110		7	0.119	0.083
	14	0.112	0.042		14	0.113	0.070
Effutu	1	0.138	0.140	OLA	1	0.128	0.103
	3	0.133	0.136		3	0.127	0.080
	5	0.132	0.120		5	0.123	0.073
	7	0.130	0.079		7	0.119	0.071
	14	0.124	0.047		14	0.114	0.061
Adisadel	1	0.141	0.138	Assin Fosu	1	0.134	0.153
	3	0.131	0.137		3	0.126	0.145
	5	0.122	0.129		5	0.122	0.116
	7	0.117	0.093		7	0.113	0.078
	14	0.108	0.083		14	0.111	0.077

Concentrations shown are the mean of 3 replicates with standard deviations within ± 0.005 ppm

Table 7 Percent removal efficiencies of AgNPs at various incubation periods

Sample sites	Days	% Co	% Pb	Sample sites	Days	% Co	% Pb
Kotokuraba	1	1.20	8.83	Ebubonku	1	3.42	11.66
	3	4.16	24.70		3	6.19	13.46
	5	6.02	32.30		5	16.43	14.43
	7	19.16	47.66		7	20.81	47.37
	14	20.58	48.32		14	21.06	49.59
Mpeasem	1	0.69	32.88	Ayikoayiko	1	3.07	1.61
	3	7.97	42.56		3	4.98	8.91
	5	11.64	62.58		5	7.81	9.38
	7	13.56	65.40		7	8.05	18.38
	14	15.45	72.55		14	8.16	24.83
Amamoma	1	3.97	9.26	Pedu	1	5.05	0.36
	3	11.31	22.68		3	7.78	17.06
	5	13.42	31.05		5	8.61	19.99
	7	16.34	40.46		7	9.29	22.21
	14	18.45	77.19		14	13.91	33.93
Effutu	1	0.45	17.94	OLA	1	2.19	0.29
	3	4.72	20.04		3	2.91	22.44
	5	4.78	29.81		5	5.60	29.73
	7	6.54	53.37		7	8.50	31.41
	14	10.46	72.63		14	12.39	40.79
Adisadel	1	0.57	0.80	Assin Fosu	1	8.14	1.38
	3	7.81	0.87		3	13.59	6.94
	5	14.21	6.50		5	15.89	25.22
	7	17.67	32.41		7	22.75	49.56
	14	23.93	40.22		14	24.02	50.63

Shown in the table are the mean values of 3 replicates with standard deviations within ± 0.05

as shown in all experimental results. This research has brought into limelight a new frontier into the applications of nanoparticles in groundwater treatment.

Conclusion

Silver nanoparticle was synthesized and characterized using UV–Vis spectrophotometer and scanning electron microscope. The UV–Vis spectra showed the characteristics surface plasmon absorption peak of 406 nm for the nanoparticle. The morphology of the nanoparticle was analyzed using scanning electron microscope which showed a mean diameter of 20 nm. The choice of silver nanoparticle in this research was due to its ease of synthesis, inexpensive starting materials, produces no sludge when used in water treatment and high metal adsorption capacity as discussed in earlier. The research presented herein showed that nanoparticles efficiencies toward metal ions removal in metal complex standard solutions are high as compared to that of groundwater. This observation we believe might be due to the complex nature of underground water samples. Nevertheless, the results indicate metal ion removal in both metal

ion complex and aqueous media is time–dependent. These observations suggest a further research into understanding the adsorption kinetics of metal ions to the surface of nanomaterials is needed.

Compliance with ethical standards

Conflict of interest The authors declare no conflict of interest.

References

Agarwal A, Joshi H (2010) Application of nanotechnology in the remediation of contaminated groundwater: a short review. Recent Res Sci Technol 2(6):51–57

Ajah KC, Ademiluyi J, Nnaji CC (2015) Spatiality, seasonality and ecological risks of heavy metals in the vicinity of a degenerate municipal central dumpsite in Enugu, Nigeria. J Environ Health Sci Eng 13(1):15

Alissawi N, Zaporojtchenko V, Strunskus T, Kocabas I, Chakravadhanula VSK (2013) Effect of gold alloying on stability of silver nanoparticles and control of silver ion release from vapor-deposited Ag–Au/polytetrafluoroethylene nanocomposites. Gold Bull 46(1):3–11. https://doi.org/10.1007/s13404-012-0073-6

Alqudami A, Munassar S, Alhemiary N (2013) The sorption properties of exploding wire prepared Ag, Fe and ZnO nanoparticles for nitrite removal from water. Int J Mater Sci (IJMSCI) 3(1):18–25

Awual MR (2016) Ring size dependent crown ether based mesoporous adsorbent for high cesium adsorption from wastewater. Chem Eng J 303:539–546

Azimi A, Azari A, Rezakazemi M, Ansarpour M (2017) Removal of heavy metals from industrial wastewaters: a review. ChemBioEng Rev 4(1):37–59

Baldoví HG, Neaţu Ş, Khan A, Asiri AM, Kosa SA, Garcia H (2015) Understanding the origin of the photocatalytic CO_2 reduction by Au- and Cu-loaded TiO_2: a microsecond transient absorption spectroscopy study. J Phys Chem C 119(12):6819–6827

Ball DW (2006) Field guide to spectroscopy, vol 8. Spie Press Bellingham, Washington

Biziuk M, Beyer A, Zukowska J (2010) Preservation and storage of water samples. In: Namiesnik J, Szefer P (eds) Analytical measurements in aquatic environments. CRC Press, Taylor & Francis Group, UK, pp 19–41

Chouler J, Cruz-Izquierdo Á, Rengaraj S, Scott JL, Di Lorenzo M (2018) A screen-printed paper microbial fuel cell biosensor for detection of toxic compounds in water. Biosens Bioelectron 102:49–56

Dasgupta N, Ranjan S, Ramalingam C (2017) Applications of nanotechnology in agriculture and water quality management. Environ Chem Lett 15(4):591–605

Ding J, Di Z, Wu D, Luan Z, Zhu Y, Li YH (2005) Adsorption thermodynamic, kinetic and desorption studies of Pb^{2+} on carbon nanotubes. Water Res 39(4):605–609

Elangovan R, Philip L, Chandraraj K (2008) Biosorption of hexavalent and trivalent chromium by palm flower (*Borassus aethiopum*). Chem Eng J 141(1–3):99–111

Eltayeb NE, Khan A (2019) Design and preparation of a new and novel nanocomposite with CNTs and its sensor applications. J Mater Res Technol 8(2):2238–2246

Federation WE, Association APH (2005) Standard methods for the examination of water and wastewater. American Public Health Association (APHA), Washington

Fu F, Wang Q (2011) Removal of heavy metal ions from wastewaters: a review. J Environ Manag 92(3):407–418

Gaur N, Flora G, Yadav M, Tiwari A (2014) A review with recent advancements on bioremediation-based abolition of heavy metals. Environ Sci Process Impacts 16(2):180–193

Ghasemzadeh G, Momenpour M, Omidi F, Hosseini MR, Ahani M, Barzegari A (2014) Applications of nanomaterials in water treatment and environmental remediation. Front Environ Sci Eng 8(4):471–482

Giri S, Qiu Z (2016) Understanding the relationship of land uses and water quality in twenty first century: a review. J Environ Manag 173:41–48

Jadhav SV, Bringas E, Yadav GD, Rathod VK, Ortiz I, Marathe KV (2015) Arsenic and fluoride contaminated groundwaters: a review of current technologies for contaminants removal. J Environ Manag 162:306–325

Jameel AA, Sirajudeen J, Vahith RA (2012) Studies on heavy metal pollution of ground water sources between Tamilnadu and Pondicherry, India. Adv Appl Sci Res 3:424–429

Khan A, Khan AAP, Hussein MA, Neppolian B, Asiri AM (2019) Preparation of new and novel wave like poly(2-anisidine) zirconium tungstate nanocomposite: thermal, electrical and ion-selective studies. Chin J Chem Eng 27(2):459–466

Kogan MJ, Bastus NG, Amigo R, Grillo-Bosch D, Araya E, Turiel A, Puntes VF (2006) Nanoparticle-mediated local and remote manipulation of protein aggregation. Nano Lett 6(1):110–115

Kunduru KR, Nazarkovsky M, Farah S, Pawar RP, Basu A, Domb AJ (2017) Nanotechnology for water purification: applications of nanotechnology methods in wastewater treatment. In: Water purification. Elsevier, pp 33–74

Larsen TA, Hoffmann S, Lüthi C, Truffer B, Maurer M (2016) Emerging solutions to the water challenges of an urbanizing world. Science 352(6288):928–933

Li YL, Liu K, Li L, Xu ZX (2012) Relationship of land use/cover on water quality in the Liao River basin, China. Procedia Environ Sci 13:1484–1493

Li H, Cheng D, Dong L, Qian F (2018) Enhancement in permselectivity and antibacterial performances of polyamide RO membranes via surface modification of AgCl nanoparticles. Desalin Water Treat 116:19–28

Madhura L, Kanchi S, Sabela MI, Singh S, Bisetty K, Inamuddin (2018) Membrane technology for water purification. Environ Chem Lett 16(2):343–365

Marcovecchio JE, Botté SE, Freije RH (2007) Heavy metals, major metals, trace elements. Handb Water Anal 2:275–311

Monteagudo JM, Ortiz MJ (2000) Removal of inorganic mercury from mine waste water by ion exchange. J Chem Technol Biotechnol 75(9):767–772

Mulfinger L, Solomon SD, Bahadory M, Jeyarajasingam AV, Rutkowsky SA, Boritz C (2007) Synthesis and study of silver nanoparticles. J Chem Educ 84(2):322

Mutamim NSA, Noor ZZ, Hassan MAA, Yuniarto A, Olsson G (2013) Membrane bioreactor: applications and limitations in treating high strength industrial wastewater. Chem Eng J 225:109–119

Odoh R, Agbaji E, Kagbu J (2011) Assessment of trace metals pollution in auto-mechanic workshop in some selected local government area of Benue State, Nigeria. Int J Chem 3(4):78

Pradeep T, Anshup (2009) Noble metal nanoparticles for water purification. Thin Solid Films 517(24):6441–6478

Qu X, Alvarez PJJ, Li Q (2013) Applications of nanotechnology in water and wastewater treatment. Water Res 47(12):3931–3946

Santhosh C, Velmurugan V, Jacob G, Jeong SK, Grace AN, Bhatnagar A (2016) Role of nanomaterials in water treatment applications: a review. Chem Eng J 306:1116–1137

Savage N, Diallo MS (2005) Nanomaterials and water purification. J Nanopart Res 7(4–5):331–342

Shankar A, Kongot M, Saini VK, Kumar A (2020) Removal of pentachlorophenol pesticide from aqueous solutions using modified chitosan. Arab J Chem 13(1):1821–1830

Shim J-Y, Gupta VK (2007) Reversible aggregation of gold nanoparticles induced by pH dependent conformational transitions of a self-assembled polypeptide. J Colloid Interface Sci 316(2):977–983

Shiri-Yekta Z, Yaftian M, Nilchi A (2013) Silica nanoparticles modified with a Schiff base ligand: an efficient adsorbent for Th(IV), U(VI) and Eu(III) ions. Korean J Chem Eng 30(8):1644

Shugar GJ, Drum DA, Lauber J, Bauman SL (2001) Environmental field testing and analysis ready reference handbook. McGraw Hill Professional, New York

Suksabye P, Thiravetyan P, Nakbanpote W (2008) Column study of chromium(VI) adsorption from electroplating industry by coconut coir pith. J Hazard Mater 160(1):56–62

Sumesh E, Bootharaju MS, Anshup, Pradeep T (2011) A practical silver nanoparticle-based adsorbent for the removal of Hg^{2+} from water. J Hazard Mater 189(1–2):450–457

Sundaram B, Feitz A, de Caritat P, Plazinska A, Brodie R, Coram J, Ransley T (2009) Groundwater sampling and analysis—a field guide. Geosci Aust Rec 27(95):104

Tiwari DK, Behari J, Sen P (2008) Application of nanoparticles in waste water treatment 1. World Appl Sci J 3(3):417–433

Vodela JK, Renden JA, Lenz SD (1997) Drinking water contaminants. Poult Sci 76(11):1474–1492

Weng C-H, Sharma YC, Chu S-H (2008) Adsorption of Cr(VI) from aqueous solutions by spent activated clay. J Hazard Mater 155(1–2):65–75

Westerhoff P, Alvarez P, Li Q, Gardea-Torresdey J, Zimmerman J (2016) Overcoming implementation barriers for nanotechnology in drinking water treatment. Environ Sci Nano 3(6):1241–1253

Yang K, Zhu L, Xing B (2006) Adsorption of polycyclic aromatic hydrocarbons by carbon nanomaterials. Environ Sci Technol 40(6):1855–1861

Yantasee W, Warner CL, Sangvanich T, Addleman RS, Carter TG, Wiacek RJ (2007) Removal of heavy metals from aqueous systems with thiol functionalized superparamagnetic nanoparticles. Environ Sci Technol 41(14):5114–5119

Zhang Y, Wu B, Xu H, Liu H, Wang M, He Y, Pan B (2016) Nanomaterials-enabled water and wastewater treatment. NanoImpact 3:22–39